

Ultrafast near-field spectroscopy of quasi-one-dimensional transport in a single quantum wire

Valentina Emiliani,* Tobias Guenther, and Christoph Lienau

Max-Born-Institut für Nichtlineare Optik und Kurzzeitspektroskopie, Max-Born-Strasse 2a, D-12489 Berlin, Germany

Richard Nötzel and Klaus H. Ploog

Paul-Drude-Institut für Festkörperelektronik, Hausvogteiplatz 5-7, D-10117 Berlin, Germany

(Received 10 January 2000; revised manuscript received 1 March 2000)

Quasi-one-dimensional carrier transport is studied in a single $\text{Al}_x\text{Ga}_{1-x}\text{As}/\text{GaAs}$ quantum wire by combining two-color femtosecond pump and probe spectroscopy and near-field optical microscopy. Evidence is found for a transient nonambipolar electron transport along the wire axis on a picosecond time and 100 nanometer length scale.

Recently the nonequilibrium dynamics of excitons and free carriers in quasi-two-dimensional semiconductor nanostructures have been extensively investigated using a variety of far-field ultrafast optical techniques.¹ This led to a detailed understanding of those processes. Much less is known about the carrier dynamics in quasi-one-dimensional (1D) systems, such as quantum wires (QWR's). Semiclassical theories predict that, in idealized 1D systems, the Coulomb scattering under strict conservation of energy and quasimomentum is strongly suppressed,² resulting, e.g., in an enhanced carrier mobility. However, in realistic systems, the effects of Coulomb quantum kinetics,³ the influences of multiple subbands (intersubband scattering), and scattering by interface and surface roughness or with acoustic and optical phonons are predicted to make the transport dynamics similar to those in quantum wells (QW's).⁴

Transport studies in QWR's have mainly been performed with electrical techniques.⁵ Only a few optical measurements are reported,^{6,7} mainly because of the limited spatial resolution that is achieved with conventional far-field microscopy. These stationary photoluminescence studies have resolved the ambipolar diffusive transport in $(\text{InP})_2/(\text{GaP})_2$ QWR arrays⁶ and single $\text{GaAs}/\text{Al}_x\text{Ga}_{1-x}\text{As}$ QWR's.⁷

Pronounced deviations from such ambipolar diffusive transport dynamics are predicted to occur for spatially and temporally strongly localized optical excitation of nanostructures.⁸ These theoretical studies predict in particular that electron and hole wave packets that are created by interband excitation above the band edge propagate basically like free particles, only weakly influenced by the Coulomb interaction. Experimentally, the observation of those dynamics requires optical techniques with ultrahigh spatial and temporal resolution. Recently, we have demonstrated that the combination of near-field microscopy and femtosecond pump-probe-spectroscopy allows one to image carrier dynamics in nanostructures with 200 nm spatial and 200 fs temporal resolution.⁹

In this paper, we use this technique for mapping the carrier transport along a single quantum wire on ultrashort length and time scales. We find, at room temperature, a surprising enhancement of the quasi-one-dimensional carrier mobility with respect to the ambipolar mobility in the embedding QW. The experiments suggest that the quasi-one-

dimensional transport reflects the nonambipolar motion of electrons that move mainly independently from the optically generated hole distribution.

Quantum wires with a thickness of up to 13 nm and embedded in a 6 nm GaAs quantum well were grown by molecular beam epitaxy on patterned GaAs (311)A substrates. The QWR/QW layer is clad between two 50 nm thick $\text{Al}_{0.5}\text{Ga}_{0.5}\text{As}$ lower and upper barrier layers. The upper barrier is covered by a 20 nm thick GaAs cap layer.¹⁰ The total 1D confinement energy of the QWR is about 80 meV (Fig. 1).¹¹ This pronounced 1D confinement gives rise to intense QWR photoluminescence (PL) at room temperature (centered around 1.46 eV), spectrally well separated from the QW PL at 1.52 eV.¹²

Spatially and spectrally resolved pump-probe experiments were performed at room temperature with pulses derived from a modelocked 80 MHz Ti:sapphire oscillator providing 50 fs pulses tunable between 810 and 870 nm. The laser

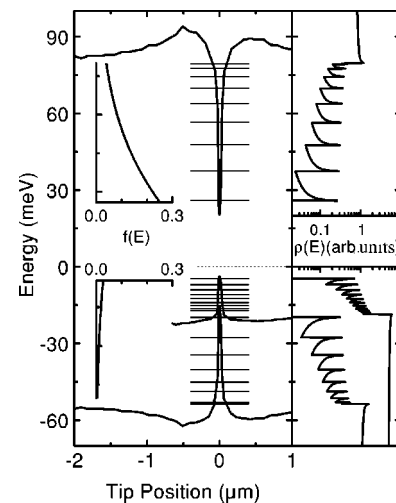


FIG. 1. Lateral confinement potential of the QWR structure, as derived from spatially resolved photoluminescence excitation spectroscopy.¹¹ The horizontal lines indicate the calculated subband energies. The insets show the density of states $\rho(E)$ in the QWR and embedding QW region and the electron and hole distribution functions $f(E)$ for localized excitation of a density of 10^{11} cm^{-2} electron-hole pairs in a 400 nm diameter spot.

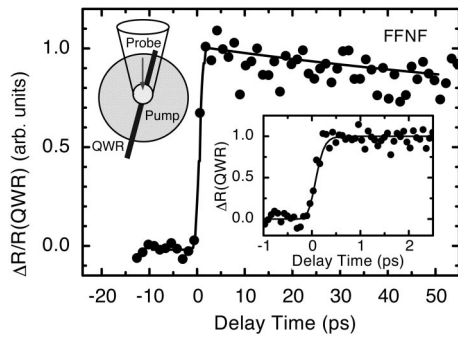


FIG. 2. Temporal variation of the pump-induced reflectivity change $\Delta R/R(QWR)$ at the QWR position on a time scale of 50 ps. The excitation is performed with a far-field spot having a diameter of $30 \mu\text{m}$ (FFNF). The pump laser is centered at 1.52 eV to create electron-hole pairs in high-lying QWR states and in the embedding QW. The probe laser at 1.46 eV probes the local bleaching of the excitonic QWR absorption. Inset: $\Delta R/R(QWR)$ within the first 3 ps.

output is split into a pump and a probe beam, each traveling through a separate prism setup for spectral shaping and group velocity dispersion compensation. Two different optical configurations are used. In a near-field pump/near-field probe geometry (NFNF), both pump and probe pulses are transmitted through the same near-field fiber probe, resulting in a subwavelength excitation spot. In a far-field pump/near-field probe geometry (FFNF), only the probe pulse is sent through the fiber while the pump is focused through a far-field lens to a spot size of about $30 \mu\text{m}$. In both configurations, the probe light reflected from the sample is collected in the far field and detected with a photodiode as a function of pump and probe time delay t_d .

First, experiments performed with far-field excitation (FFNF) are presented (Fig. 2). The carrier-induced change in local reflectivity $\Delta R/R$ is probed with pulses of 11 meV bandwidth tuned to the QWR resonance at 1.46 eV . The pump laser (bandwidth 40 meV) is centered at 1.52 eV and spectrally shaped in order to overlap the absorption spectrum of the QW (excitation density $\approx 10^{11} \text{ cm}^{-2}$). Carriers are generated in high-energy QWR states and in the embedding QW. The QWR contribution $\Delta R/R(QWR)$ to the overall reflectivity change $\Delta R/R$ is extracted by taking the difference of the transients measured at the QWR location and out of the QWR region.⁹ The temporal evolution of $\Delta R/R(QWR)$ shows a fast initial rise within 200 fs, the time resolution of the experiment, and a constant value up to $t_d = 55 \text{ ps}$. A similar evolution of $\Delta R/R(QWR)$ is observed for resonant far-field excitation of the QWR at 1.47 eV and probing at energies of high-lying QWR states around 1.51 eV (not shown).

Different dynamics are observed when both pump and probe pulses are transmitted through the near-field fiber probe (NFNF), as shown in Fig. 3. The spectra of the pump and probe lasers are shown in the inset. The transient of Fig. 3 reveals now a clear decay by more than 50% on a time scale of 50 ps—in contrast to the time-independent reflectivity change for far-field excitation. Similar dynamics are observed for probe energies between 1.5 eV and 1.43 eV (Fig. 4)—i.e., by tuning the probe energy through the QWR resonance—and for resonant QWR excitation.

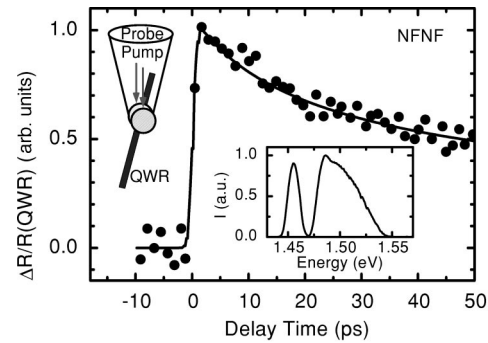


FIG. 3. Temporal variation of the pump-induced reflectivity change $\Delta R/R(QWR)$ at the QWR position on a time scale of 50 ps for localized near-field excitation with a spatial resolution of less than 400 nm (NFNF). The decay of the reflectivity signal reflects the carrier transport along the QWR. The solid line shows a simulation of a 1D diffusion model with $D_{QWR} = 80 \text{ cm}^2/\text{s}$. Inset: spectra of pump and probe lasers, centered at 1.50 and 1.46 eV , respectively.

The pump-induced change in the probe reflectivity, $\Delta R/R(QWR)$, arises from the carrier-induced bleaching of the excitonic QWR absorption.⁹ This bleaching is due to photoexcited carriers inside the QWR and, thus, $\Delta R/R(QWR)$ is an efficient probe for the temporal evolution of the QWR carrier density. There are two mechanisms that contribute to this excitonic QWR nonlinearity: Coulomb screening and phase-space filling. In quantum wells, at high temperatures and for carrier densities that are similar to our experimental conditions, phase-space filling dominates and causes a direct reduction of the exciton oscillator strength.¹³ The observed spectral dependence of $\Delta R/R(QWR)$ (Ref. 9) identifies phase-space filling as the dominant contribution to the exciton QWR nonlinearity as well. The phase-space filling and therefore also the magnitude of the bleaching of the excitonic QWR absorption and of $\Delta R/R(QWR)$ are probes of the sum of the local concentrations of electrons and holes within the QWR region. The observation of a reflectivity change for probe energies around 1.46 eV thus requires carrier redistribution from optically excited high lying QWR and continuum states to the bottom of the QWR. The absence of any slower dynamics on the transient in Fig. 2 suggests that this redistribution process occurs within the first

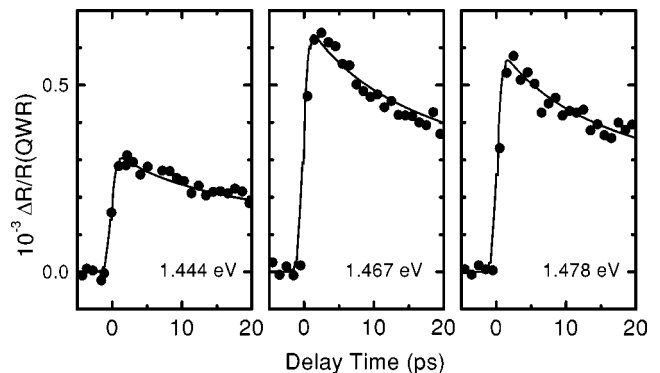


FIG. 4. Probe wavelength dependence of $\Delta R/R(QWR)(t_d)$ for localized near-field excitation with a spatial resolution of less than 400 nm (NFNF) for probe lasers centered at 1.444 eV , 1.467 eV , and 1.478 eV , respectively. Excitation conditions as in Fig. 3.

200 fs. At room temperature and under our excitation conditions this relaxation involves a complex scattering scenario with contributions from both carrier-LO phonon scattering (typical phonon emission times in QWR's are ≥ 150 fs)^{3,4} and carrier-carrier scattering. The ultrafast rise in reflectivity that is observed when the pump is tuned in resonance with the QWR absorption and the probe wavelength is set to high-lying QWR states, suggests that a thermalized carrier distribution is formed within the first 200 fs, similar to the thermalization dynamics in quantum wells.

On a time scale of up to 50 ps, the dynamics observed in the two configurations are clearly different: In the FFNF configuration, after the initial fast rise, the signal remains constant up to 55 ps. This suggests that, after the thermalization of the carrier distribution in the QWR region, there is no significant change in the carrier concentration in this region of the sample. In this geometry, a spatially nearly homogeneous carrier distribution is excited. Therefore, in the embedding QW, the local gradients in the carrier concentration in the direction perpendicular to the QWR axis are weak. Diffusive ambipolar transport of carriers within the embedding QW (for which a RT diffusion coefficient of $D_{QW}=12$ cm²/s was measured in our sample¹²) does not significantly enhance the QWR carrier density on a ps time scale. The carrier distribution is also homogeneous along the QWR, so that quasi-one-dimensional transport is not expected to affect the reflectivity signal, which decays by electron-hole recombination with a decay time of 1.9 ns.¹² In the NFN configuration we observe, on the contrary, a clear decay of the reflectivity change on a 10 ps time scale. Here, the excitation and probe pulse, spatially overlapping, are localized to a small spot of about 400 nm in diameter. Therefore, the optically injected carriers can migrate out of the excitation volume. This results in a decrease of the local carrier concentration and thus in a reduction of the pump-induced reflectivity change. In general, the transport of carriers out of the excited volume can occur both along the QWR wire as well as perpendicular to it. In these experiments, a density of about 10^{11} cm⁻² electron-hole pairs is locally generated in a 400 nm diameter spot. The data in Fig. 2 suggest that a quasi-equilibrium Fermi distribution in both QWR and QW states is formed within 200 fs. The density of states $\rho(E)$ and distribution functions $f(E)$ for electrons and holes in such a nondegenerate distribution are schematically depicted in Fig. 1. The Fermi levels are about 10 meV and 90 meV below the energy of the lowest QWR subband for the electrons and holes, respectively. Due to the difference in confinement potentials for electrons (65 meV) and heavy holes (15 meV) the spatial distributions of electrons and holes are different. The density of electrons in the QWR is estimated to be about 4 times higher than the QWR hole density. A large fraction of the photoexcited electrons is confined inside the QWR while most of the holes are populating quasi-continuum states of the embedding QW. Thus $\Delta R/R(\text{QWR})$ probes mainly the local dynamics of electrons inside the QWR. Also, for electrons, the probability for occupation of high-lying QWR states f_e , from which transport in the lateral direction, i.e., into the unexcited embedding QW can occur, is small—about 1/8 of f_e in the lowest subband of the QWR. Considering this small fraction of carriers, and taking into account the ambipolar QW diffusion coefficient $D_{QW}=12$ cm²/s, one

finds a negligible contribution of the lateral transport to the transients in Fig. 3. We conclude that the decay of the reflectivity transient in Fig. 3 reflects mainly the transport of electrons along the QWR axis.

Assuming that the transport along the QWR—on a time scale of several picoseconds—is adequately represented within a 1D-diffusion model, the experimental curves can be simulated, having the diffusivity as the only unknown parameter. Carrier diffusion and recombination can be described by the following equation:

$$\frac{\partial n(x,t)}{\partial t} = -\frac{n(x,t)}{\tau} + G(x,t) + D\frac{\partial^2 n(x,t)}{\partial x^2}, \quad (1)$$

where n is the 1D carrier concentration, τ the recombination lifetime, $G(x,t)$ the generation rate, and D the diffusion coefficient. Its solution is

$$\Delta n(x,t) = \frac{\Delta n(x,t)_o}{(4\pi Dt)^{1/2}} \exp\left(\frac{-x^2}{4Dt}\right) \exp(-t/\tau). \quad (2)$$

Here, $\Delta n(x,t)_o$ is the initial carrier concentration, given by the pump laser profile. To simulate the observed time evolution, $\Delta n(x,t)$ has to be convoluted with the shape of the probe pulse, taken as a Gaussian of full width at half maximum, $spot$, estimated from the measured spatial resolution R : $spot = R\sqrt{2}$. The observed carrier concentration $\Delta n(x,t)_{obs}$ is then:

$$\Delta n(x,t)_{obs} = \frac{\Delta n(x,t)_o}{\pi} \sqrt{\frac{\pi}{W+4Dt}}, \quad (3)$$

where $W = spot^2/(4\ln 2)$. The observed decay of the QWR reflectivity is well described by taking a quasi-one-dimensional diffusion coefficient $D_{QWR} = 80 \pm 20$ cm²/s (solid lines in Fig. 3 and Fig. 4). This value of the 1D diffusion coefficient is more than 5 times larger than the ambipolar 2D diffusion coefficient $D_{QW} = 12$ cm²/s. The 2D value, using the Einstein relation $\mu = eD/k_bT$ (e electron charge, k_bT thermal energy), corresponds to a mobility of 500 cm²/V s which is close to the mobility of holes in GaAs at 300 K. At room temperature, hole diffusion governs the ambipolar transport through the QW and the hole mobility is limited by scattering with phonons via the optical deformation potential.¹⁴ 2D QW mobilities have been optically measured in our sample in the temperature range between 10 and 300 K,¹⁵ and are in good agreement with mobility measurements reported for GaAs/Al_xGa_{1-x}As QW's.¹⁶ At high temperatures, these data show only a weak dependence of the mobility on the well width, varying by about a factor of 2 as the well width is changed from 4 to 15 nm. Theoretically, the well width dependence of the deformation potential scattering rates results mainly from the variation in the density of states and this suggests that, in thin QW's, the RT mobility increases linearly with well width.¹⁷ In our sample, the local thickness of GaAs QWR increases to about two times that of the embedding QW, and we thus expect the ambipolar RT diffusion within the two regions to be similar within a factor of 2.

On the contrary, we find experimentally a significantly larger diffusion coefficient $D_{QWR} = 80 \pm 20$ cm²/s. This

value corresponds to a mobility $\mu = 3000 \text{ cm}^2/\text{Vs}$, which is close to the RT mobility of electrons in GaAs.¹⁸

This suggests that, in our experiments, the transport of electrons along the QWR axis is strongly different from a conventional ambipolar diffusive transport regime, with a spatially and temporally correlated motion of electrons and holes and a mobility that is hole limited.¹⁹ Instead, we observe a rapid motion of electrons out of the excitation volume, along the QWR axis, with a mobility that is basically unaffected by the hole distribution within the QWR. This suggests that, due to the excess density of electrons in the QWR that is created with spatially and temporally localized excitation, and the pronounced spatial gradient of the electron density along the QWR, the electrostatic repulsion between electrons in the QWR is not compensated by the Coulomb attraction between electrons and holes. Thus, the electrons can propagate mainly independently from the hole distribution and this gives rise to the observed enhancement of the 1D mobility.

This conclusion is supported by the finding that, probing

the temporal evolution of the carrier-induced bleaching of the excitonic QW reflectivity $\Delta R/R(\text{QW})$ on the QW flat area, we observe a significantly less pronounced decay on a 20 ps time scale.²⁰ This decay is in agreement with a quasi-two-dimensional ambipolar QW diffusion with a diffusion coefficient $D_{\text{QW}} = 12 \text{ cm}^2/\text{s}$.

In conclusion, we have imaged the nonequilibrium carrier dynamics in a single quantum wire at room temperature by combining femtosecond pump-and-probe spectroscopy and near-field microscopy. Evidence is found for a transient non-ambipolar transport of electrons along the quantum wire on a picosecond time and 100 nm length scale, that is attributed to an ultrafast spatial separation of electron and hole densities.

One of the authors (V.E.) gratefully acknowledges the TMR program for financial support under the proposal ERB4001GT975127. This work has been financially supported by the Deutsche Forschungsgemeinschaft (SFB296) and the European Union (EFRE). We thank Thomas Elsaesser and Michael Woerner for stimulating discussions.

*Author to whom correspondence should be addressed. Electronic address: emiliani@mbi-berlin.de

¹ J. Shah, *Ultrafast Spectroscopy of Semiconductors and Semiconductor Nanostructures* (Springer, Berlin, 1999).

² H. Sakaki, *Jpn. J. Appl. Phys., Part 2* **19**, L735 (1980).

³ F. Prengel and E. Scholl, *Phys. Rev. B* **59**, 5806 (1998).

⁴ See, e.g., L. Rota, *Phys. Rev. B* **52**, 5183 (1995).

⁵ See, e.g., A. Yacoby *et al.*, *Phys. Rev. Lett.* **77**, 4612 (1996).

⁶ Y. Tang, D. H. Rich, A. M. Moy, and K. Y. Cheng, *Appl. Phys. Lett.* **72**, 55 (1998).

⁷ Y. Nagamune, H. Watabe, F. Sogawa, and Y. Arakawa, *Appl. Phys. Lett.* **67**, 1535 (1995).

⁸ F. Steininger, A. Knorr, T. Stroucken, P. Thomas, and S. W. Koch, *Phys. Rev. Lett.* **77**, 550 (1996).

⁹ T. Guenther, V. Emiliani, F. Intonti, C. Lienau, T. Elsaesser, R. Nötzel, and K. H. Ploog, *Appl. Phys. Lett.* **75**, 3500 (1999).

¹⁰ R. Nötzel, M. Ramsteiner, J. Menniger, A. Trampert, H.-P. Schönherr, L. Däweritz, and K. H. Ploog, *Jpn. J. Appl. Phys., Part 2* **35**, L297 (1996).

¹¹ Ch. Lienau, A. Richter, G. Behme, M. Süptitz, D. Heinrich, T.

Elsaesser, M. Ramsteiner, R. Nötzel, and K. H. Ploog, *Phys. Rev. B* **58**, 2045 (1998).

¹² A. Richter, G. Behme, M. Süptitz, Ch. Lienau, T. Elsaesser, M. Ramsteiner, R. Nötzel, and K. H. Ploog, *Phys. Rev. Lett.* **79**, 2145 (1997).

¹³ S. Hunsche, K. Leo, H. Kurz, and K. Kohler, *Phys. Rev. B* **49**, 16 565 (1994).

¹⁴ D. J. Wolford, G. D. Gilliland, T. F. Kuech, J. A. Bradley, and H. P. Hjalmarson, *Phys. Rev. B* **47**, 15 601 (1993).

¹⁵ A. Richter, M. Süptitz, Ch. Lienau, T. Elsaesser, M. Ramsteiner, R. Nötzel, and K. H. Ploog, *J. Microsc.* **194**, 393 (1999).

¹⁶ See, e.g., H. Hillmer *et al.*, *Phys. Rev. B* **39**, 10 901 (1989).

¹⁷ B. K. Ridley, *J. Phys. C* **15**, 5899 (1982).

¹⁸ Sadao Adachi, *GaAs and Related Materials* (World Scientific, Singapore, 1994).

¹⁹ The observed fast carrier relaxation into the QWR within less than 200 fs excludes the possibility that the high 1D mobility can be explained by a 1D reduction in the scattering rates.

²⁰ T. Guenther *et al.* (unpublished).